

Toxicology Research

Accepted Manuscript



This is an *Accepted Manuscript*, which has been through the Royal Society of Chemistry peer review process and has been accepted for publication.

Accepted Manuscripts are published online shortly after acceptance, before technical editing, formatting and proof reading. Using this free service, authors can make their results available to the community, in citable form, before we publish the edited article. We will replace this *Accepted Manuscript* with the edited and formatted *Advance Article* as soon as it is available.

You can find more information about *Accepted Manuscripts* in the [Information for Authors](#).

Please note that technical editing may introduce minor changes to the text and/or graphics, which may alter content. The journal's standard [Terms & Conditions](#) and the [Ethical guidelines](#) still apply. In no event shall the Royal Society of Chemistry be held responsible for any errors or omissions in this *Accepted Manuscript* or any consequences arising from the use of any information it contains.

The cellular toxicology of mitragynine, the dominant alkaloid of the narcotic-like herb, *Mitragyna speciosa* Korth

Nor Aini Saidin¹, Elaine Holmes, Hiromitsu Takayama² and Nigel, J. Gooderham

Computational and Systems Medicine, Faculty of Medicine, Sir Alexander Fleming Building, Imperial College London, SW7 2AZ, UK and ² Graduate School of Pharmaceutical Sciences, Chiba University, Chiba, Japan.

Please address correspondence to:

Dr Nigel J Gooderham
Computational and Systems Medicine,
Faculty of Medicine,
Sir Alexander Fleming Building,
Imperial College London,
London
SW7 2AZ, UK

Email: n.gooderham@imperial.ac.uk

Tel: (44) 020 7594 3188

Fax: (44) 020 7594 3050

Key words: *Mitragyna Speciosa*; mitragynine; opiate; cytotoxicity; drug abuse.

¹Current address:

Advanced Medical and Dental Institute, Universiti Sains Malaysia, Bertam, 13200
Kepala Batas, Pulau Pinang, Malaysia

ABSTRACT

Mitragyna speciosa Korth (*Kratom*), a herb of the Rubiaceae family is indigenous to southeast Asia. The plant and its dominant alkaloid mitragynine (MIT) are narcotic/analgesic and illicit consumption is widespread in Asia; the toxicological consequences of consumption are poorly documented. We determined cytotoxicity of MIT on human cell lines and report dose and time-dependent stimulation and inhibition of proliferation. Since MIT has powerful opiate-like activity, we focussed on human neuronal SH-SY5Y cell line and found the colony forming ability of cells treated with MIT showed a dose-dependent trend for reduced survival. Studies using metabolically competent MCL-5 cells and chemical inhibitors indicated that CYP 2E1 and 2A6 were involved in the cytotoxicity. Cytotoxicity was preceded by cell cycle arrest mainly at G1 and S phase. To assess whether arrest was due to DNA damage or mutation, we examined genotoxic potential using the L5178 tk^{+/-} mouse lymphoma assay and found that MIT was not genotoxic at the tk locus, even at doses that were highly cytotoxic. To investigate mechanisms of MIT cytotoxicity, we used flow cytometry and annexin V with 7-amino-actinomycin D staining and show apoptosis and necrotic activity. Apoptosis was further supported as MIT rapidly induced the activity of executioner caspases 3/7. However, cytotoxicity of MIT was partially reduced by inclusion of the opioid receptor antagonist naloxone, a μ and δ opioid receptor antagonist, suggesting that cytotoxicity depends in part on opioid signalling, consistent with the known toxicity of other opiates. Based on consumption of 20 leaves/day of *Mitragyna speciosa*, we estimated daily human exposure to MIT to be about 17 mg MIT for regular consumers, potentially giving plasma concentrations in of 10^{-9} to 10^{-7} M. Importantly, fatalities after kratom consumption have been reported to occur in individuals with blood mitragynine concentrations of between 0.45-1.0 μ M, substantially lower than the threshold of toxicity predicted from this *in vitro* report. Clearly the implications of these findings to humans consuming *Mitragyna speciosa* leaves will require further study, but individuals taking large quantities of these opiate-like materials may be at risk, especially those who have a high CYP2E1 activity, such as heavy alcohol users.

INTRODUCTION

The use of traditional medicines from natural products, mainly plants, is increasing in developing countries. Although the safety and efficacy of most of the traditional medicines used in humans are yet to be thoroughly investigated, people still turn to them due to availability and cost. *Mitragyna speciosa* Korth, also known as 'kratom', is a traditional plant having unique therapeutic constituents; it is found growing in Malaysia, Thailand and neighbouring countries. *Mitragyna speciosa* Korth plant, especially its leaves, has long been consumed by local farmers and labourers who chew the fresh leaves, smoke the dry leaves or drink as a tea suspension¹ or even eat it in the form of resin, for stimulant effects. The plant has unique dual opioid properties which exert a stimulant effect at low doses and sedative and analgesic effects at the higher doses in humans^{2, 3}. This characteristic of the plant has led to it being highly abused by drug addicts⁴. The chemistry and pharmacology of the leaves of this plant, especially the dominant alkaloid, mitragynine (MIT, Figure 1), is known to include opioid-like agonistic effects^{1, 5, 6}. MIT was reported to exert antinociceptive and anti-tussive effects upon oral, subcutaneous and intraperitoneal administration to rodents⁷. Recently the MIT congener, 7-hydroxymitragynine was found to have potent opioid-like effects both *in vitro* and *in vivo*⁸. In contrast to this established pharmacology, the toxicological consequences of exposure to these compounds are poorly documented. Drug addicts using the plant and its extracts report dry mouth, emaciated body with an unhealthy complexion (dry skin and dark lips, resembling hepatic face), frequent urination, constipation coupled with small and blackish stools, loss of appetite and weight loss, central nervous system depression, reduced smooth muscle tone and for heavy users, prolonged sleep^{2, 3}. In Malaysia, the possession of any form of the plant by the public is illegal. However, in other parts of the world, kratom is currently not scheduled. The availability of kratom over the internet has attracted use of the plant as self-treatment in opioid withdrawal and chronic pain⁴. Recently, there have been several reported fatalities associated with consumption of Kratom⁹⁻¹¹. The reason for these deaths is not understood but MIT toxicity is implicated. In view of this and the lack of understanding of the toxicity of MIT, we have examined the cytotoxicity potential of MIT, the dominant alkaloid of *Mitragyna speciosa* in human cell lines and the mechanisms involved in this toxicity.

MATERIALS AND METHODS

Chemicals.

Pure mitragynine (>98% purity) was prepared from *Mitragyna speciosa* as previously described⁶ and identity confirmed by comparison to an authentic reference sample (from the Institute of Medical research, Kuala Lumpur, Malaysia). Mitragynine (>98%) was dissolved in ethanol and filtered through sterile 0.45 µM filter for cell culture studies. Metabolic inhibitors diethylthiocarbamate (DED), a CYP 2A6 inhibitor and 3-amino-1,2,4-triazole (ATZ), a CYP 2E1 inhibitor were purchased from Sigma-Aldrich Company (Poole, England). For flow cytometry analysis, Alexa Fluor® 647-Annexin V conjugate staining kit, 7-Amino-actinomycin D (7-AAD) dye and HEPES buffer were obtained from Invitrogen, U.K. The opioid receptor antagonists, naloxone, naltrindole and cyprodime hydrobromide were purchased from Sigma-Aldrich, U.K. For the caspase studies, the Apo One® Homogenous Caspase 3/7 kit was purchased from Promega, U.K. The fluorescent dye, 2,7-dichlorofluorescein diacetate (DCFH-DA) and hydrogen peroxide (H₂O₂) for ROS assay were purchased from Sigma-Aldrich, U.K.

Cell line and conditions.

The SH-SY5Y and HEK 293 cell lines were purchased from the European Collection of Cell Cultures (Salisbury, UK) and the MCL-5 cell line was purchased from Gentest Corp. (MA, USA). The mouse lymphoma L5178Y TK[±] cells were a kind gift from Dr M O'Donovan AstraZeneca (Macclesfield, UK). MCL-5 cells, a metabolically competent human lymphoblastoid cell line stably transfected with plasmids encoding CY1A2, 2A6, 2E1, 3A4, epoxide hydrolase and constitutive 1A1 were cultured in RPMI 1640; HEK 293, a human embryo kidney cell line was cultured in high glucose Dulbecco's modified Eagle's medium (DMEM) and SH-SY5Y cells, a human neuroblastoma cell line was cultured in high glucose Glutamax® DMEM. All media were from Invitrogen Corporation (Paisley, Scotland, UK). MEM, DMEM and Glutamax® DMEM media were supplemented with 10% fetal bovine serum (FBS), 2mM L-glutamine and 100 units of penicillin/streptomycin, all from Invitrogen. RPMI 1640 was supplemented with 9% horse serum, 2 mM L-glutamine, 2mM histidinol and 100 units of penicillin/streptomycin, also from Invitrogen. Routinely, cells were maintained at 37°C, in a humidified atmosphere of 95%/5% air/CO₂. Adherent cell lines, HEK 293 and SH-SY5Y cells were harvested by trypsinisation with trypsin-

EDTA (Invitrogen) and centrifugation, and subcultured appropriately; suspension cell lines, MCL-5 cells were harvested by centrifugation. Histidinol (2 mM) was added to every subculture of MCL-5, for plasmid maintenance.

Cell viability (Trypan blue exclusion assay).

In order to estimate the percentage of dead cells after treatment with MIT, cells were harvested then stained with trypan blue solution (0.4%) and the number of trypan blue-positive (dead cells) and trypan blue negative (live) cells were counted with a haemocytometer under a light microscope.

In some experiments, the role of opioid receptors in mediating MIT toxicity was investigated; three opioid receptor antagonists were used; naloxone (1 μ M, μ and δ opioid antagonist), naltrindole (1 μ M, δ opioid antagonist) and cyprodime hydrobromide (1 μ M, μ opioid antagonist).

Colony survival (clonogenicity assay).

For survival studies, cells (SH-SY5Y and HEK 293 cells) treated with MIT, were trypsinised, centrifuged and seeded at 100 cells per well in 6 well plates in 2 ml drug-free medium and incubated for a period of 6-7 days. The wells were stained with methylene blue (1% in 50% methanol) and colonies that contained 50 or more cells were scored as survivors. Relative cell survival was expressed as percentage of appropriate vehicle-treated controls. In some experiments, the effect of metabolic activation on MIT cytotoxicity was also examined using using Arochlor-induced rat liver S9 (9 μ g protein).

Flow cytometry analysis (cell cycle analysis).

Treated SH-SY5Y cells were harvested by routine trypsinisation, washed with PBS and fixed in ice-cold 70% ethanol overnight. The fixed cells were then collected by centrifugation (1200 r.p.m. for 5 min) and re-suspended in staining solution containing 5 mg/ml propidium iodide (PI), 10 μ g/ μ l RNase and 0.1% triton-x100 and incubated at 37°C for 30 minutes. Samples were analysed using the Cellquest Pro software on a Becton Dickinson FACSCalibur flow cytometer. For each sample, 30,000 events were collected and aggregated cells were gated out of the analysis.

The percentage of cells at different phases of the cell cycle was determined using ModFit LT MAC 3.1 software. PI was excited at 488 nm, and the fluorescence analysed at 620 nm.

Immunoblot analysis.

Cell lysates (10 µg protein) were resolved by SDS-polyacrylamide gel electrophoresis and electroblotted onto nitrocellulose membrane. Blots were blocked by incubation in 5% low fat dried milk in 25 mM phosphate buffered saline and 0.1% tween 20 for 45 minutes at room temperature. The nitrocellulose blot was incubated with primary antibody overnight at 4°C, followed by secondary antibody conjugated to horseradish peroxidase for 1 hr at room temperature. Detection was achieved using ECL kit (Amersham Life Science, UK). The antibodies against p53 (1 in 2000 dilution) were purchased from Santa Cruz, (California, USA) and the β-actin antibody (1 in 20,000 dilution) was purchased from Sigma-Aldrich (Poole, England). The quantitation of each immunoblot obtained was carried out using a UMAX powerlook 1100 scanner, and the p53 band intensity normalised to β-actin was analysed using Image J version 1.37 software.

The L5178Y TK^{+/-} mouse lymphoma cell assay.

The mouse lymphoma L5178Y TK^{+/-} cells were maintained in RPMI 1640 Glutamax-1 medium containing 3.0 mM L-glutamine and 25 mM HEPES and supplemented with 1.8 mM sodium pyruvate, 50 µg/ml streptomycin: 50 IU/ml penicillin, 0.1% pluronic F-68 and 10%(v/v) heat inactivated donor horse serum. The cells were treated prior to use in the assay with thymidine (9 µg/ml), hypoxanthine (15 µg/ml), methotrexate (0.3 µg/ml) and glycine (22.5 µg/ml) to maintain a low and stable background mutant frequency. 7,12-Dimethylbenz[a]anthracene (DMBA) was used as positive control in the presence of aroclor induced rat liver S9-mix at a final concentration of 5 µg/ml, dissolved in DMSO. Methyl methanesulfonate (MMS) dissolved in dimethyl sulphoxide was used as a positive control in the absence of S9-mix at final concentration of 20 µg/ml. The assay was performed in a 96 well plate format as described by Clements¹² and Moore *et al.*,¹³. After treatment with MIT (3h in the presence of aroclor induced rat liver S9 or 24 h in the absence of S9), cells were harvested. Treated cells (10⁶) were suspended in normal culture media for 48 h to permit expression of the tk^{-/-} phenotype. An aliquot of cell suspension was then

plated out for viability in a 96 well plate at a density of 1.6 cells per well. For mutant selection, trifluorothymidine was added to the cell suspension to give a final concentration of 4 mg/ml, cells were added to each well of a 96 well plate at a density of 2000 cells per well. The plates were incubated for 12 days at 37°C in a humidified atmosphere of 5% CO₂. At the end of this period, wells containing no viable cells were identified and counted. The mutant frequency (MF), plating efficiency and relative total growth (RTG) were determined as previously described^{12, 13}.

Annexin V conjugates/7-AAD double staining for apoptosis detection

Double staining for cellular DNA using Alexa Fluor® 647-Annexin V conjugate staining kit and 7-AAD were performed following manufacturer's instruction. SH-SY5Y cells (1×10^6) in exponential growth phase were incubated for 2 hours or overnight, and treated with various concentrations of MIT and further incubated at 37°C (5% CO₂) for 24 hour. After harvesting, cell pellets were washed with cold PBS followed by centrifugation (1200 r.p.m.). Cells were re-suspended in Annexin-binding buffer (10mM HEPES, 150 mM NaCl and 2.5 mM CaCl₂ at pH 7.4) and then counted and the cell density adjusted to 1×10^6 cells/ml. Alexa Fluor® 647-Annexin V conjugate (5 µl) was added to each 100 µl of assay and incubated at room temperature in the dark for 15 min. The Annexin-binding buffer (200 µl) was added to the suspension and kept on ice followed by adding 2 µl/100 µl cells suspension of the 7-AAD (1 mg/ml in phosphate buffer). The cells were then incubated on ice for 5 minutes until data acquisition with a Becton Dickinson FACSCalibur flow cytometer using CellQuest Pro software. The fluorescence of AlexaFluor®647- Annexin V conjugate was measured at 650 nm excitation and 665 nm emission and 7-AAD at 488 nm excitation and 620 nm emission. Thirty thousand (30,000) cells were analysed for each treatment using FLOW JO 8.1.1 software.

Apo One® homogenous caspase 3/7 assay

SH-SY5Y cells (10^5 cells/ well of six well plates) were treated with MIT for 4 hr or 18 hr. After incubation, cells were harvested by trypsinisation and centrifugation. The assay was performed according to the manufacturer's instructions (Promega, USA). After cell counting, 20,000 cells in 100 µl volume were transferred to 96 well black plates. One hundred microliter of caspase 3/7 reagents (mixture of caspase substrate and caspase buffer) was added to each well, shaken for 30 seconds and incubated

at room temperature. Serial fluorescence readings were performed over at least 1 h using a plate reader at 485 nm excitation and 520 nm emission.

Reactive oxygen species (ROS) analysis

ROS assay was carried out using SH-SY5Y cells and the fluorescent dye 2,7-dichlorofluorescein diacetate (DCFH-DA). This dye diffuses through the cell membrane and is hydrolysed enzymatically by intracellular esterases to form monofluorescent dichlorofluorescein (DCFH) in the presence of ROS. The intensity of the fluorescence is proportional to the levels of intracellular ROS¹⁴. Briefly, SH-SY5Y cells (2×10^3 cells/well) in 24 well plates were cultured overnight, then the medium was aspirated and washed with PBS to remove all traces of albumin (a free-radical quencher). PBS (2 ml) was added to each well followed by freshly prepared DCFH-DA dye dissolved in DMSO (10 μ L of 100 μ M) under subdued lighting. In some experiments, anti-oxidant, N-acetyl-L-cysteine (NAC) (5mM) was also added. After 30 minutes, cells in each well were treated with H₂O₂ (positive control) or MIT and the fluorescence was measured using a plate reader with 485 nm excitation and 530 nm emission. Fluorescence readings were continually read at 10 min intervals for up to 1 hr period.

Statistical analysis.

One way Analysis of variance (ANOVA) with Tukey-Kramer or Dunnet post tests was conducted to calculate significant differences where p-values of <0.05 were considered significant.

RESULTS

Cell viability by trypan blue exclusion assay.

MIT treated cells showed stimulation and inhibition of cell proliferation that was dose and time-dependent in the human cell lines examined (HEK 293, MCL-5 and SH-SY5Y cells) (Figure 2); SH-SY5Y and MCL-5 cells were more sensitive to the treatments (Table 1). At low doses, proliferation was stimulated in the SH-SY5Y cell line at the 24 and 48 h time points; this was less pronounced in the HEK293 cell line. The reason for the increased proliferative response is not clear and it should be noted that there was considerable variability in the data. By 72 h this stimulatory effect was no longer apparent. As the dose was increased, toxicity became more evident, particularly in the SH-SY5Y cells where survival was negligible at the highest dose employed, irrespective of incubation period. The effect of CYP expression on MIT proliferation and toxicity (trypan blue uptake) was examined in metabolically competent MCL-5 cells. In preliminary experiments, ketoconazole (CYP 3A4 inhibitor at 25 μ M), diethyldithiocarbamate (DED) (CYP 2A6 inhibitor at 100 μ M), 3-amino-1,2,4-triazole (ATZ) (CYP 2E1 inhibitor at 25 μ M) and α -naphthoflavone (CYP 1A inhibitor at 25 μ M) were incubated with MCL-5 cells and MIT. Only DED and ATZ were found to alter MIT cytotoxicity (data not shown), therefore, the effect of DED and ATZ on MCL-5 proliferation and cytotoxicity was examined in more detail (Fig. 2C). Both ATZ and DED reduced toxicity at 50 μ M MIT. At 100 μ M MIT, ATZ showed some inhibition of toxicity, although this was not statistically significant and DED was without effect.

Colony survival (clonogenicity assay).

The clonogenicity assay is a longer term measure that assesses not only the effects of cell death but also the ability of cells to form a colony. As shown in Figure 2D, under these conditions, the inhibition of proliferation by MIT is overcome on prolonged culture and colony formation although there was a significant trend for clonogenic cytotoxicity with increasing dose ($p < 0.05$ for trend). Interestingly, an increased clonogenic response of the SH-SY5Y cells at low dose MIT (0.3 μ M) was observed, although this effect was not statistically significant.

Assessment of cell cycle distribution by flow cytometry.

To determine whether MIT treatment could affect the progression of cell cycle, treated cells were stained with propidium iodide and analysed by flow cytometry. The DNA profiles of SH-SY5Y cells were assessed after exposure to various concentrations of MIT (Figure 3). There were no major effects on the cycle seen with doses up to 30 μM MIT for 24 hr. However, striking changes were evident at the highest dose tested, 75 μM MIT, where cells accumulated at G1 phase and the population appeared to shift to increased fluorescence (right shift), consistent with treated cells taking up more PI dye (Figure 3).

Mouse lymphoma thymidine kinase (tk^{-/-}) gene mutation assay

In view of the striking effect on cell cycle at 75 μM , we investigated the ability of MIT to damage DNA and induce mutation using the mouse lymphoma tk assay. The results are shown in table 2. For this assay, a positive result is described as a MF that is higher than the sum of Mean Control MF (77×10^{-6}) plus the standard global evaluation factor for this microplate assay (GEF, 126×10^{-6} , Moore et al.¹³). In the presence of S9, there was a slight increase in mutant frequency with the two highest doses, but the mutant frequency remained within the GEF and is therefore not considered to be a mutagenic response. The positive control DMBA gave a clear positive response. There was very little toxicity, assessed as the RTG, noted under these conditions. In the absence of S9 during a 24 h incubation, MIT was dose dependently cytotoxic. Cytotoxicity as measured by the RTG was substantial at the highest dose. Again, there was a small dose dependent increase in the mutant frequency, but still within the GEF and thus the compound was not considered to be mutagenic. Again the positive control, MMS, gave a clear positive response.

Immunoblot analysis.

Since the cytotoxicity of MIT was accompanied by cell cycle arrest, it was proposed that these changes could be a result of alteration in the expression and activation of regulatory proteins such as p53. Therefore, the effects of MIT on p53 protein levels were assessed in SH-SY5Y cells. Between doses of MIT, there was little difference in the expression of p53, however at all concentrations of MIT there appeared to be a loss of p53 expression compared to the control group (Figure 4).

Annexin V conjugate assay for apoptosis detection

Our preliminary observations on the toxicity of MIT indicated that MIT induced cell morphology changes indicative of apoptosis with microscopic evidence of chromatin condensation, in SH-SY5Y cells. We therefore explored the mechanisms of MIT-induced cell death. Translocation of phosphatidylserine to the outer plasma membrane indicates early apoptotic cell death, and Annexin V reactivity can be used as a marker for apoptotic cells^{15, 16}. The cells become reactive with Annexin V prior to the loss of the ability of the plasma membrane to exclude the dye 7-AAD and thus detection of unaffected (live) cells, early apoptotic, necrotic and late apoptotic cells is possible¹⁷.

The cell populations were gated according to four different quadrants (Figure 5); Q1 represent live cells (exclude Annexin V and 7-AAD), Q2 are Annexin V positive indicating early apoptosis, Q3 are Annexin V and 7-AAD positive indicating late apoptosis/necrosis and Q4 represent necrotic cells permeable to the 7-AAD dye.

With MIT treatment at the highest concentration tested, 75 μ M, it appears that the profile was shifted to the right side with concomitant increase of cells in Q2, Q3 and Q4 indicating increased apoptotic and necrotic cells. This increased susceptibility to dye permeability is consistent with the response observed during cell cycle analysis using PI staining.

Involvement of executor caspases (3 and 7)

The activity of caspase 3/7 was assessed in SH-SY5Y cells treated with MIT. With incubation of MIT for either 4 or 18 hrs, at 100 μ M and 300 μ M MIT, there was significant activation of caspase 3/7 activity (Figure 6).

ROS generation in SH-SY5Y cells treated with MIT

An important mechanism whereby xenobiotics induce cell death is through the generation of reactive oxygen species (ROS). Intracellular ROS can be detected using the formation of the fluorescent product DCFH after hydrolysis of DCGH-DA. As shown in figure 7, the positive control, H₂O₂ generated a clear response in the SH-SY5Y cell that was inhibited by pre-incubation (30 min prior to addition of H₂O₂) with NAC. Similar treatments with MIT failed to induce any detectable ROS response in this cell (Figure 7).

Effects of opioid receptor antagonists on treated SH-SY5Y cells

We considered the possibility that the toxicity of MIT may be associated with interaction at the opiate receptor. The SH-SY5Y cells express predominantly the μ and δ opioid receptor¹⁸. We therefore used a trypan blue assay to assess cytotoxicity effects of MIT in the presence of selective opioid receptor antagonists naloxone (μ and δ antagonist), naltrindole (δ antagonist) and cyprodime hydrobromide (μ antagonist).

After 24 hr of treatment, naloxone at the concentration of 1 μ M successfully inhibited cytotoxicity that is evident at 100 μ M MIT (Figure 8). In contrast naltrindole failed to offer significant protection against MIT induced cytotoxicity and cyprodime hydrobromide was only partially protective (Figure 8).

DISCUSSION

The analgesic properties of *Mitragyna speciosa* plant have been described *in vitro* and *in vivo*, mainly using crude alkaloid extracts but also with its dominant alkaloid mitragynine (MIT) and congeners^{19, 20}. These medicinal properties have been reported for extracts of the leaves of this plant but not from other species of *Mitragyna*. Several countries like Thailand, Myanmar, Malaysia and Australia have made possession of the plant illegal, due to its narcotic properties, yet preparations of the plant are available for sale over the internet. The popularity of this herb in Western culture is increasing and some individuals are now taking it for self-treatment of chronic pain and as an aid to opioid withdrawal⁴. The potential toxicity of MIT and of other products derived from *Mitragyna speciosa* is currently poorly documented and recently there have been several reported fatalities associated with consumption of Kratom⁹⁻¹¹. The reason for these deaths is not understood but MIT toxicity is implicated. Therefore an *in vitro* toxicological assessment of its dominant alkaloid MIT was undertaken. MIT was found to exert dose-dependent cytotoxic effects to human cell lines. We demonstrated that MIT was toxic to all three cell lines

examined and the human neuronal SH-SY5Y cell was chosen for further study as neuronal tissue is a high probability target for opiate-like compounds such as MIT. The concentration of MIT required to reduce the relative (to control) cell number by 50% (IC_{50}) following 24 hr treatment of SH-SY5Y cells was 7.5×10^{-5} M. In contrast, we noted that low doses of MIT (3×10^{-7} M) stimulated cell proliferation during the first 48 h but this effect was lost at the 72 h time point. The reason for this stimulation of proliferation is not clear, especially since other classical opiate agonists, such as morphine, suppress rather than stimulate proliferation²¹.

Many xenobiotics undergo metabolic activation in the process of exerting their cytotoxicity effects. CYP proteins are key enzymes involved in oxidative xenobiotic metabolism, therefore we examined if metabolism was involved in MIT cytotoxicity using MCL-5 cells (metabolically competent and express-CYP1A1, 1A2, 2A6, 2E1, 3A4 and human epoxide hydrolase). We compared the toxicity of MIT in MCL-5 cells in the presence of inhibitors of the CYP enzymes. Incubations in the presence of inhibitors of CYP3A4 and 1A1 failed to affect toxicity, but inhibitors of 2E1 and 2A6 did protect against MIT toxicity, suggesting involvement of these enzymes.

To further characterise the nature of the cytotoxicity of MIT, we examined SH-SY5Y cell cycle distribution, using flow cytometry^{16, 17}. SH-SY5Y cells treated with MIT appeared to be resistant to cell cycle effects except at the highest dose tested, 75 μ M, where there was evidence for a G1 arrest. An unexpected observation in these experiments was the right-shifting of the DNA profiles which was pronounced in the high dose of MIT. This phenomenon implies that the cells have taken up more PI, thus increasing the DNA staining intensity. The explanation for this phenomenon is unknown however, it could reflect plasma membrane integrity being compromised by the treatment, thus creating pores or increased membrane permeability.

In view of the effect on cell cycle at 75 μ M, we investigated the ability of MIT to damage DNA and induce mutation using the well-established L5178 tk^{+/-} mouse lymphoma cell assay. Under the conditions of the ICH agreed guidelines for this assay, MIT was not found to be genotoxic in the presence or absence of a metabolic activation system, although substantial toxicity was noted at the 75 μ M concentration when RTG was lowered to 17%.

Since the cytotoxicity of MIT was accompanied by cell cycle arrest, it was proposed that these changes could be a result of alteration in the expression and activation of regulatory proteins such as p53. In fact immunoblotting indicated the loss of the P53 protein with MIT treatment. The mechanism of this loss is not obvious, but could involve compromised membrane integrity. Consistent with this, the right shift of the DNA profiles (increased PI staining) in the flow cytometry experiments indicates a mechanism in which the dyes could diffuse more easily into the cell.

Further flow cytometry analysis using double staining with Annexin V conjugates and 7-AAD supported this MIT-induced membrane permeability, with the dyes being more readily taken up by treated cells. These experiments further indicated that most of the treated cells were necrotic and late apoptotic populations.

The ability of cysteine proteases, caspases^{22, 23} to perform proteolytic cleavage at defined aspartate acid residues in various cellular substrates is an established marker of apoptosis²⁴. We examined the involvement of executioner caspases (caspase 3 and 7) in MIT cytotoxicity in SH-SY5Y cells and found significant increases in caspases 3 and 7 activities at both concentrations of MIT tested. This finding suggests that the mode of the cell death of MIT treated cells involves caspase 3 and 7 activation pathway and is indicative of apoptosis.

Under normal circumstances, the low levels of ROS generated by mitochondria as a normal by-product of oxygen metabolism are usually removed by an abundance of endogenous free radical scavengers such as enzyme superoxide dismutases, glutathione and other cellular antioxidants such as ascorbic acid and vitamin E^{25, 26}. However xenobiotic insult, which causes mitochondrial malfunctions, may lead to generation of ROS in higher levels thus triggering oxidative stress, lipid peroxidation and finally cell death. In the present study, MIT treatment failed to induce ROS, suggesting this was not a mechanism of the apoptotic cell death noted here.

MIT has been shown to exert its biological activities via opioid receptors mainly μ - and δ - and to a lesser extent κ -opioid receptors^{5, 27 28}. The opioid analgesic, morphine is also known to exert its biological activities mainly via μ -opioid and also δ -

and κ -opioid receptors²⁹ however the selective binding site of MIT for μ -receptor is reported to be of a different subtype from morphine⁵. Cell death induced by opioids is associated with their opioid receptor signalling, such as neuronal apoptosis induced by morphine due to opioid receptor desensitisation and uncoupling to pertussis toxin (PTX)-sensitive inhibitory G protein (Gi)³⁰. Additionally, morphine has been shown to induce cell cycle block and apoptosis in MCF-7 and MDA-MB231 mammary cancer cells that was naloxone sensitive³¹; inhibited growth and proliferation and induced cell cycle arrest in MGC-803 gastric cells³²; inhibited proliferation and increased apoptosis of neural progenitor cells that was reversed by naloxone, and the authors suggested the involvement of the μ opioid receptor³³. Thus this information poses the question of whether the opioid receptors mediating the biological activity of the *Mitragyna speciosa* Korth plant may also mediate the MIT induced toxicity or cell death. Opiate receptor antagonists should therefore protect against MIT induced cell death. As anticipated, naloxone (μ - and δ -receptor antagonist) and cyprodime hydrobromide (μ - receptor antagonists) successfully gave protection against MIT toxicity. Interestingly the opiate agonist etorphine (exhibits activity through the μ , κ and δ opioid receptors) inhibited the cell growth of SK-N-SH cells, yet the inhibition was not prevented by naloxone, suggesting that the effects of etorphine might not be mediated by a classical opioid receptor³⁴. These observations indicate that further work is required to define the mechanisms involved in the toxicity of MIT.

Based on consumption of 20 leaves/day of *Mitragyna speciosa*, the estimated daily human exposure to MIT is about 17 mg for regular consumers³. Assuming total body distribution of the drug (70 kg BW/person), *in vivo* concentrations are probably in order of 10^{-9} to 10^{-7} M MIT. Extrapolating cell based *in vitro* studies to whole animal studies require huge assumptions, but since the *in vitro* toxicity of MIT is not obvious until ≥ 75 μ M, human consumption of *Mitragyna speciosa* Korth leaves at pharmacologically active doses would appear to be substantially lower than the threshold of toxicity predicted from this *in vitro* study. However, these assumptions do not take into account local concentrations of MIT in the GI tract after consumption, which could be significantly higher. The reported GI disturbance noted in Kratom addicts could reflect this potential toxicity and there have been several reports of fatalities associated with kratom consumption⁹⁻¹¹. In these reports, the blood

concentrations of MIT ranged from 0.48 – 1.5 μM , which is fifty fold lower than the concentrations required to produce overt toxicity in the present *in vitro* toxicity study. Additionally, the study by McIntyre et al⁹ reported that liver concentrations of MIT (1.08 μM) were twice the blood levels. Although these reported fatalities were complicated by the detection of other drug entities, MIT was implicated as contributing to the deaths.

Conclusions

Based on the current findings MIT has potential to cause cytotoxicity to mammalian cells. Since MIT is the dominant alkaloid found in *Mitragyna speciosa* Korth (Kratom), human addiction to Kratom is potentially harmful. The main target system of MIT pharmacology is the central nervous system and our studies with the human neuroblastoma cell line SH-SY5Y indicate that such cells are susceptible to MIT cytotoxicity, although MIT was found to exert dose dependant cytotoxicity effects in all human cell lines examined.

The cytotoxicity events are initially seen as cell cycle arrest then proceed to cell death with increasing dose of MIT. In addition, the metabolism studies also suggest that CYP 2E1 and possibly 2A6 activity appeared to be involved in MIT cytotoxicity. From the human perspective, if *Mitragyna speciosa* leaves were to be ingested by individuals with elevated CYP 2E1 activity such as high consumers of alcohol, the toxicity of *Mitragyna speciosa* leaves and extracts could be potentiated. This is potentially of significance since the local concentration of MIT in the GI tract after consumption of *Mitragyna speciosa* is likely to be higher than systemic exposure; an additional susceptibility factor is that the GI tract is known to express CYP2E1. This is consistent with the GI disturbance noted amongst Kratom addicts. Of particular importance is the reported fatalities associated with kratom consumption, where the blood concentrations of MIT were in the μM range. This is significantly lower than the levels of MIT required to induce toxicity we report here in our *in vitro* mechanistic studies and clearly the potential for MIT to cause toxicity *in vivo* warrants further investigation.

ACKNOWLEDGEMENT

We would like to thank Ministry of Higher Education of Malaysia and International Islamic University Malaysia for funding this project.

REFERENCES

1. K. L. Jansen and C. J. Prast, *Journal of ethnopharmacology*, 1988, **23**, 115-119.
2. K. Grewal, *British Journal of Medicinal Psychology*, 1932, **12**, 41-58.
3. S. Suwanlert, *Bulletin on narcotics*, 1975, **27**, 21-27.
4. E. W. Boyer, K. M. Babu and G. E. Macalino, *The American journal on addictions / American Academy of Psychiatrists in Alcoholism and Addictions*, 2007, **16**, 352-356.
5. S. Thongpradichote, K. Matsumoto, M. Tohda, H. Takayama, N. Aimi, S. Sakai and H. Watanabe, *Life sciences*, 1998, **62**, 1371-1378.
6. H. Takayama, *Chemical & pharmaceutical bulletin*, 2004, **52**, 916-928.
7. E. Macko, J. A. Weisbach and B. Douglas, *Archives internationales de pharmacodynamie et de therapie*, 1972, **198**, 145-161.
8. K. Matsumoto, Y. Hatori, T. Murayama, K. Tashima, S. Wongseripipatana, K. Misawa, M. Kitajima, H. Takayama and S. Horie, *European journal of pharmacology*, 2006, **549**, 63-70.
9. I. M. McIntyre, A. Trochta, S. Stolberg and S. C. Campman, *Journal of analytical toxicology*, 2015, **39**, 152-155.
10. M. F. Neerman, R. E. Frost and J. Deking, *Journal of forensic sciences*, 2013, **58 Suppl 1**, S278-279.
11. R. Kronstrand, M. Roman, G. Thelander and A. Eriksson, *Journal of analytical toxicology*, 2011, **35**, 242-247.
12. J. Clements, *Mutation research*, 2000, **455**, 97-110.
13. M. M. Moore, M. Honma, J. Clements, G. Bolcsfoldi, M. Cifone, R. Delongchamp, M. Fellows, B. Gollapudi, P. Jenkinson, P. Kirby, S. Kirchner, W. Muster, B. Myhr, M. O'Donovan, J. Oliver, T. Omori, M. C. Ouldelhkim, K. Pant, R. Preston, C. Riach, R. San, L. F. Stankowski, Jr., A. Thakur, S. Wakuri, I. Yoshimura and W. Mouse Lymphoma Assay, *Mutation research*, 2003, **540**, 127-140.
14. F. Galvano, A. Russo, V. Cardile, G. Galvano, A. Vanella and M. Renis, *Food and chemical toxicology : an international journal published for the British Industrial Biological Research Association*, 2002, **40**, 25-31.
15. M. van Engeland, L. J. Nieland, F. C. Ramaekers, B. Schutte and C. P. Reutelingsperger, *Cytometry*, 1998, **31**, 1-9.
16. H. Zhu, A. R. Boobis and N. J. Gooderham, *Cancer Res*, 2000, **60**, 1283-1289.
17. Z. Darzynkiewicz, X. Li and E. Bedner, *Methods in cell biology*, 2001, **66**, 69-109.
18. S. M. Kazmi and R. K. Mishra, *Biochemical and biophysical research communications*, 1986, **137**, 813-820.
19. K. Matsumoto, M. Mizowaki, T. Suchitra, H. Takayama, S. Sakai, N. Aimi and H. Watanabe, *Life sciences*, 1996, **59**, 1149-1155.
20. K. Watanabe, S. Yano, S. Horie and L. T. Yamamoto, *Life sciences*, 1997, **60**, 933-942.
21. D. Agarwal and J. A. Glasel, *Cell proliferation*, 1999, **32**, 215-229.
22. S. M. Srinivasula, A. Saleh, M. Ahmad, T. Fernandes-Alnemri and E. S. Alnemri, *Methods in cell biology*, 2001, **66**, 1-27.
23. E. S. Alnemri, D. J. Livingston, D. W. Nicholson, G. Salvesen, N. A. Thornberry, W. W. Wong and J. Yuan, *Cell*, 1996, **87**, 171.

24. S. M. Srinivasula, R. Hegde, A. Saleh, P. Datta, E. Shiozaki, J. Chai, R. A. Lee, P. D. Robbins, T. Fernandes-Alnemri, Y. Shi and E. S. Alnemri, *Nature*, 2001, **410**, 112-116.
25. R. Yazdanparast and A. Ardestani, *Journal of medicinal food*, 2007, **10**, 667-674.
26. I. Fridovich, *Annals of the New York Academy of Sciences*, 1999, **893**, 13-18.
27. S. Tsuchiya, S. Miyashita, M. Yamamoto, S. Horie, S. Sakai, N. Aimi, H. Takayama and K. Watanabe, *European journal of pharmacology*, 2002, **443**, 185-188.
28. M. Tohda, S. Thongpraditchote, K. Matsumoto, Y. Murakami, S. Sakai, N. Aimi, H. Takayama, P. Tongroach and H. Watanabe, *Biological & pharmaceutical bulletin*, 1997, **20**, 338-340.
29. A. D. Corbett, G. Henderson, A. T. McKnight and S. J. Paterson, *British journal of pharmacology*, 2006, **147 Suppl 1**, S153-162.
30. I. Tegeder, S. Meier, M. Burian, H. Schmidt, G. Geisslinger and J. Lotsch, *Brain : a journal of neurology*, 2003, **126**, 1092-1102.
31. I. Tegeder, S. Grosch, A. Schmidtko, A. Haussler, H. Schmidt, E. Niederberger, K. Scholich and G. Geisslinger, *Cancer Res*, 2003, **63**, 1846-1852.
32. Y. Qin, J. Chen, L. Li, C. J. Liao, Y. B. Liang, E. J. Guan and Y. B. Xie, *Asian Pacific journal of cancer prevention : APJCP*, 2012, **13**, 1377-1382.
33. D. Willner, A. Cohen-Yeshurun, A. Avidan, V. Ozersky, E. Shohami and R. R. Leker, *PloS one*, 2014, **9**, e103043.
34. D. L. Yin, X. H. Ren, Z. L. Zheng, L. Pu, L. Z. Jiang, L. Ma and G. Pei, *Neuroscience research*, 1997, **29**, 121-127.

FIGURES

Figure 1 The structure of Mitragynine

Figure 2 Cytotoxicity of MIT treated cells.

- A. Proliferation of HEK 293 cells with MIT treatment.
 - B. Proliferation of SH-SY5Y cells with MIT treatment.
 - C. Proliferation of MCL-5 cells treated with MIT and DED (100 μ M) or ATZ (25 μ M) for 48 hr.
 - D. Clonogenicity of SH-SY5Y cells after MIT treatment for 24 h.
- Cell number was assessed using Trypan blue exclusion and clonogenicity by counting colonies. Values are the mean \pm SEM of three or four independent cultures. * $P < 0.05$ vs respective MIT alone controls, ANOVA with Tukey-Kramer post test.

Figure 3 Effects of MIT on the cell cycle distribution of SH-SY5Y cells.

Cells were treated for 24 h with MIT. Representative histograms are shown and values of each phase of the cell cycle are the mean of the three independent experiments.

Figure 4 P53 expression in SH-SY5Y cells treated with MIT for 24 h.

A representative immunoblot is shown. For quantitation, bars are normalised to the β -actin controls and are the mean of three independent experiments with SEM.

Figure 5 Flow cytometry assessment of apoptosis and necrosis of SH-SY5Y cells after 24 hr treatment with MIT.

Treated cells were stained with Alexa Fluor® 647-Annexin V conjugate and 7-AAD. Four quadrants (Q) representing normal cells (Q1), early apoptosis cells (Q2), late apoptotic/necrotic cells (Q3) and necrotic cells (Q4). Table shows mean \pm SEM values of % cells in each quadrant from 3 independent cultures ** Significantly different from respective control, $P < 0.01$, ANOVA with Dunnet post test.

Figure 6 Activity of executor caspases 3/7 in SH-SY5Y cells treated with MIT for 4 hr or 18 hr incubation.

Values are mean \pm SEM for 3 independent cultures. Significantly different from respective control, ** $P < 0.01$, ANOVA with Dunnet post test.

Figure 7 Measurement of ROS with DCFH-DA in SH-SY5Y cells treated with H2O2, or MIT with or without NAC.

Fluorescent readings are normalised to the respective control group. Values are mean \pm SEM for 3 independent cultures.

Figure 8 Trypan blue exclusion assay of SH-SY5Y cells after 24 hr treatment with A) MIT \pm Naloxone (N), B) MIT \pm Naltrindole (Nalt), C) MIT \pm Cyprodime hydrobromide (C).

Values are mean \pm SEM for 3 independent cultures. Significantly different from respective control, * $P < 0.05$, ANOVA with Bonferroni post test.

Table 1. Effect of MIT on cell growth.

IC ₅₀	
Cell line	MIT (μMolar)
SH-SY5Y	75
HEK 293	240
MCL-5	80

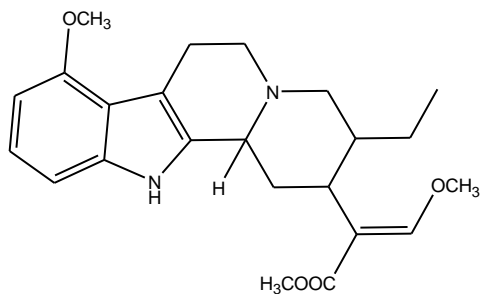
IC₅₀ values are the concentration required to reduce the relative (to control) cell number by 50% after 24 hr treatment with MIT. The values were interpolated from cell survival curves.

Table 2. Genetic toxicology of MIT in L5178 tk^{+/−} mouse lymphoma cells

Substance	Concentration (μM)	RTG ^a	Mutants ^b tk ^{−/−} (MF)
3 h incubation +S9			
MIT	0	100	77
	12.5	99	72
	25l	91	71
	50	96	106
	75	92	101
DMBA (positive control)	1 μg/ml	78	550
24 h incubation (no S9)			
MIT	0	100	88
	12.5	74	56
	25	81	104
	50	37	167
	75	17	114
MMS (Positive control)	5 μg/ml	87	590

^a RTG Relative total growth (%) – measure of cell growth relative to control.

^b MF mutant frequency (tk^{−/−} mutants per 10⁶ clone forming cells)



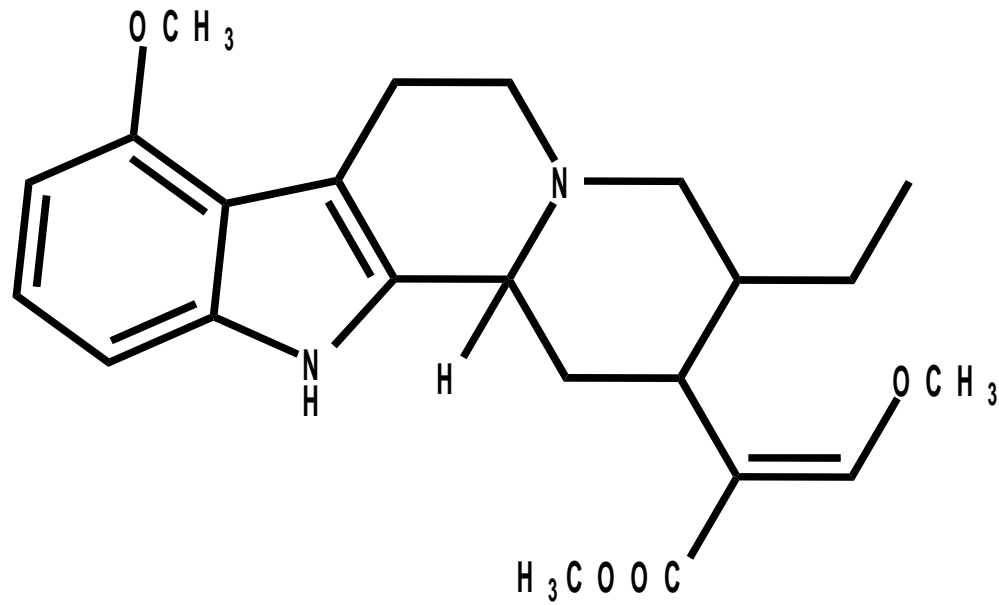
Opiate receptor?

Cycle arrest

Apoptosis

The cytotoxicity of mitragynine, the dominant alkaloid of the narcotic-like herb, *Mitragyna speciosa* Korth (Kratom) involves cell cycle arrest, apoptosis and opiate receptors.

Figure 1



Mitragynine

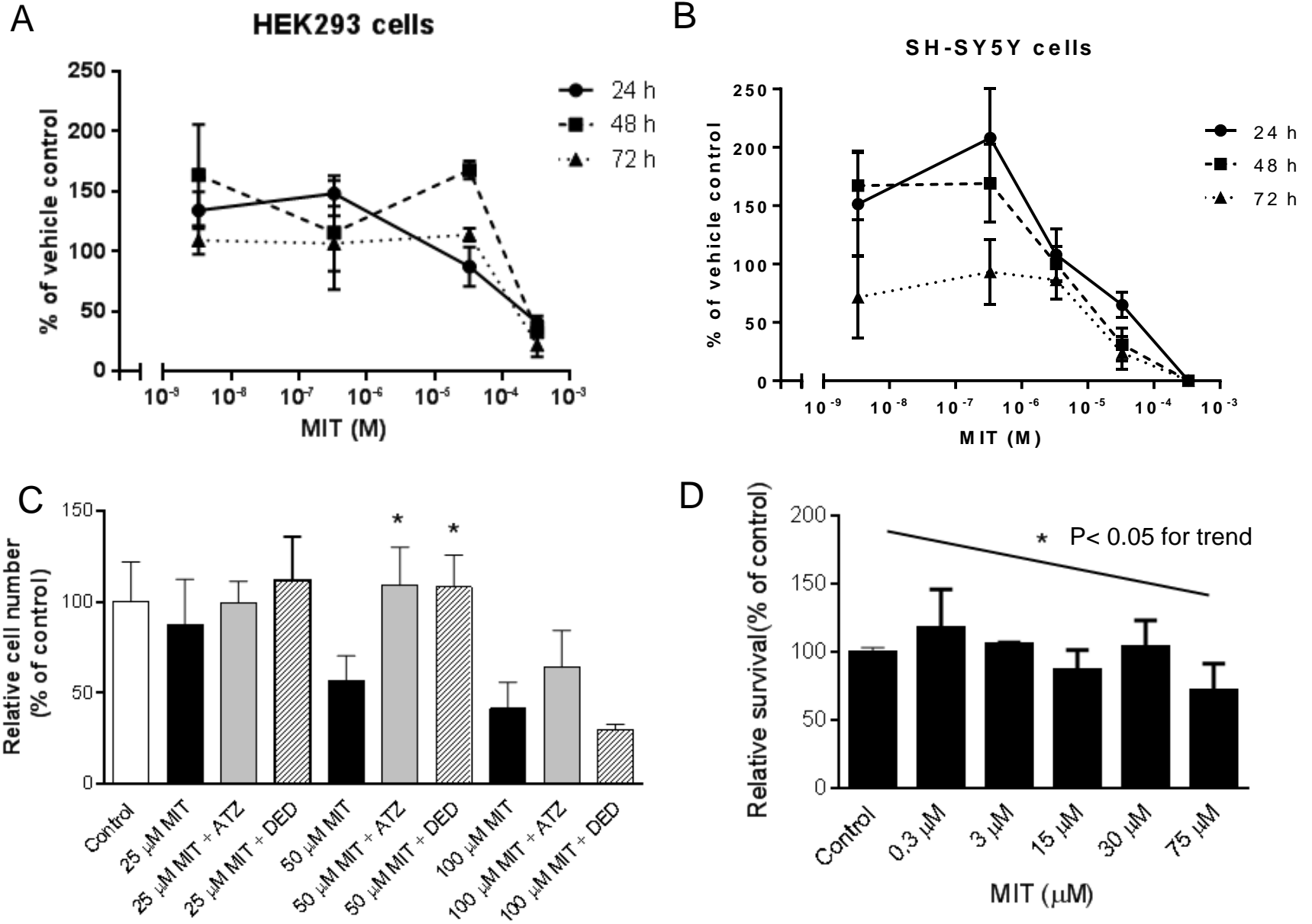


Figure 3

MIT for 24 h

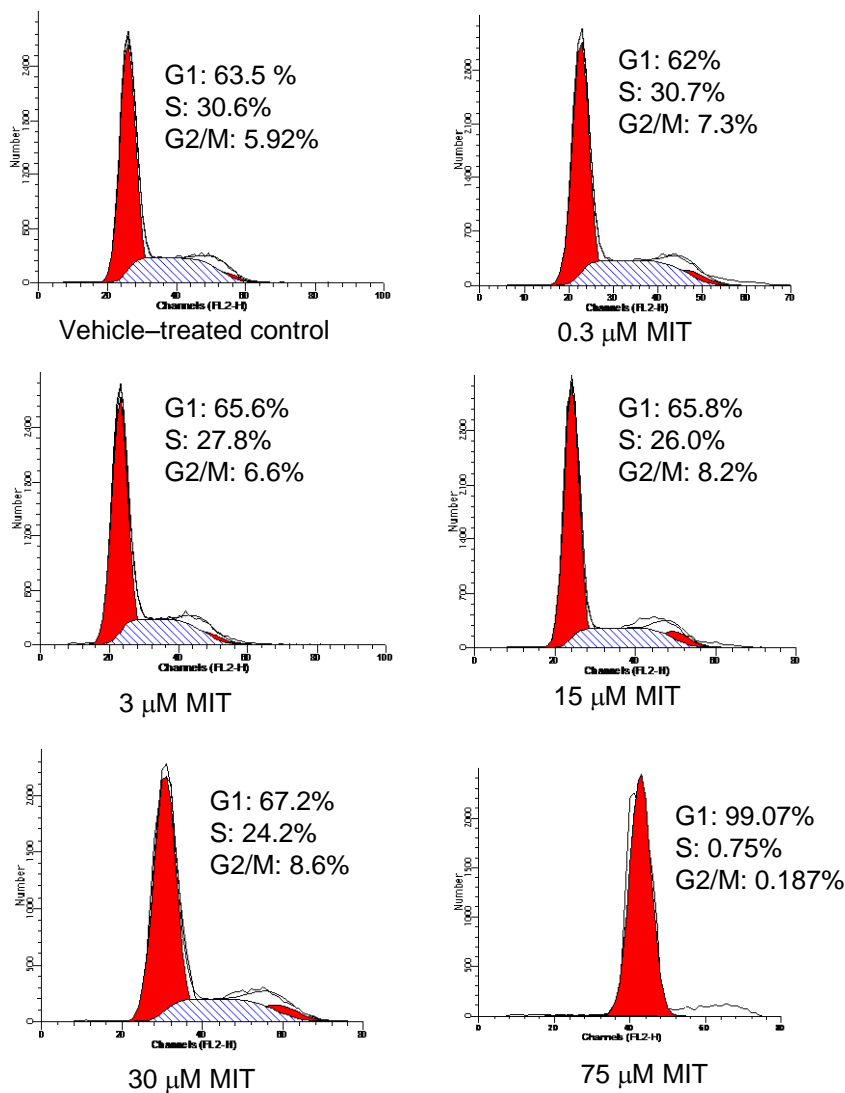


Figure 4

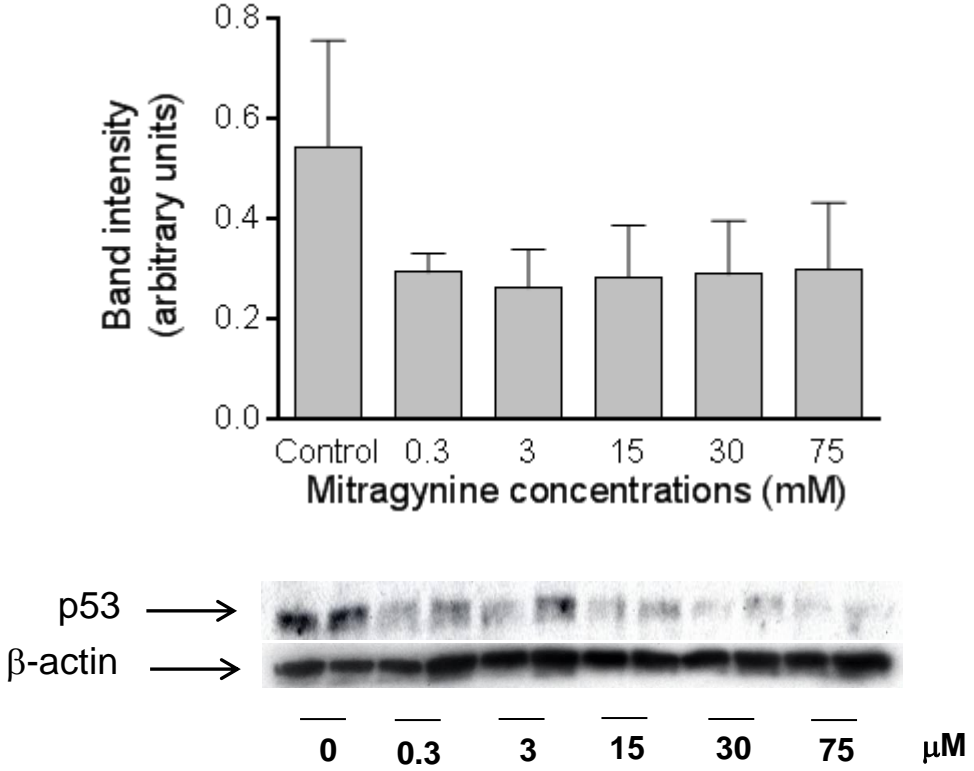
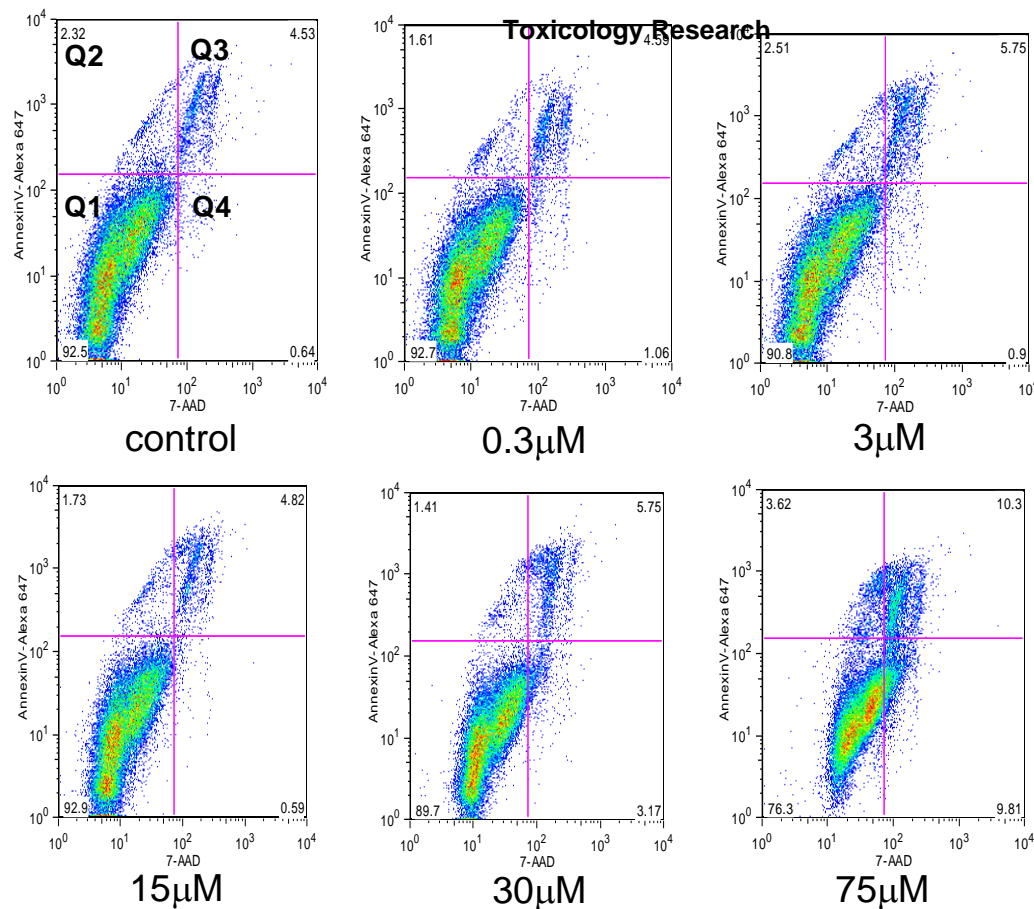


Figure 5



MIT (μM)	Q1 (%)	Q2 (%)	Q3 (%)	Q4 (%)
Control	91.3 ± 1.25	1.95 ± 0.23	5.36 ± 0.94	1.4 ± 0.56
0.3	91.9 ± 0.6	1.8 ± 0.13	5.09 ± 0.36	1.21 ± 0.27
3	90.8 ± 0.43	1.97 ± 0.3	5.92 ± 0.33	1.26 ± 0.18
15	92.2 ± 0.47	1.57 ± 0.09	4.97 ± 0.3	1.27 ± 0.34
30	89.9 ± 1.1	1.37 ± 0.04	5.94 ± 0.63	2.84 ± 0.5
75	78.4 ± 1.42**	2.3 ± 0.65	9.3 ± 0.5**	9.9 ± 0.95**

Figure 6

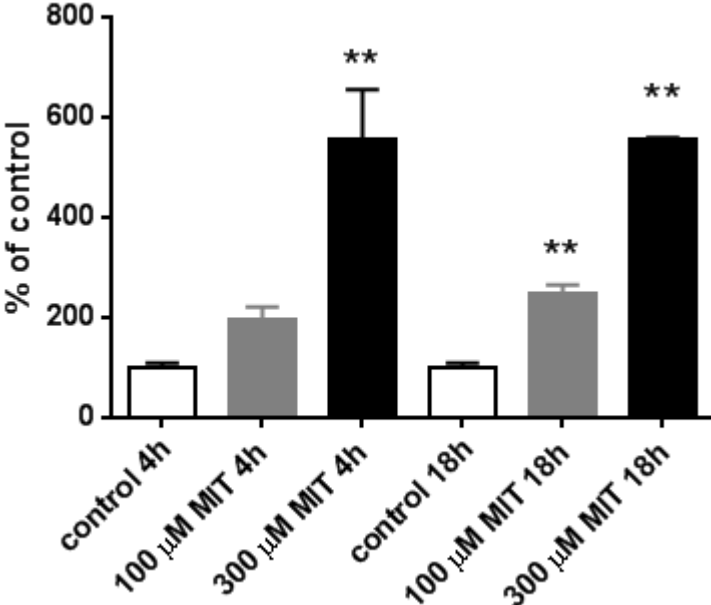


Figure 7

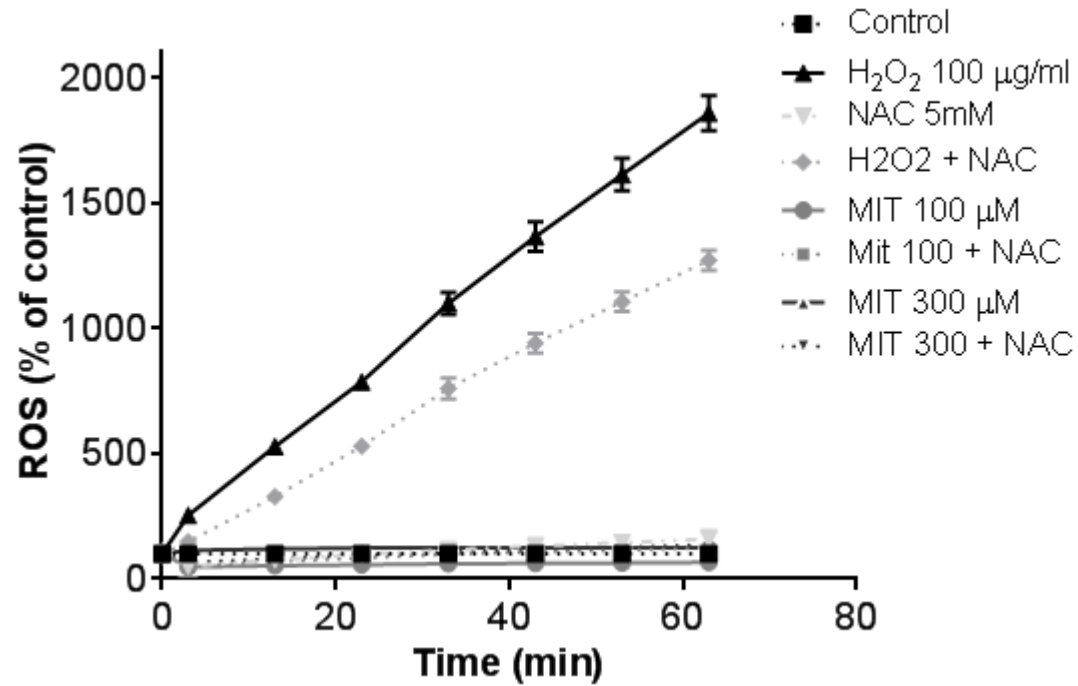


Figure 8

